

The Nonequilibrium Region of a Mixing Layer

M. A. Badri Narayanan* and S. Raghup†
Indian Institute of Science, Bangalore, India
and

E. G. Tulapurkara‡
Indian Institute of Technology, Madras, India

Experiments were conducted in the nonequilibrium region of a free mixing layer with unequal freestream velocities. Four velocity ratios $U_1/U_2 = 0.32, 0.46, 0.74$, and 0.96 —were used in this investigation. The growth of the shear layer as well as the velocity adjustment in the near wake were examined. There was reasonable agreement between the measured mean velocity profiles and those computed using the $K-\epsilon$ turbulence model. Some periodic turbulence velocity fluctuations were observed in the mixing layer, but their frequency remained the same along the flow.

Introduction

THE two-stream turbulent mixing layer is of fundamental importance in fluid mechanics. This subject is also of considerable importance in aeronautical engineering, since the wakes behind aircraft and turbine blades involve turbulent mixing. Because of the complexity of the problem, for the sake of convenience, the free mixing layer is categorized into two regimes, namely the near wake and far wake. In the far wake, the flow is dominated by large-scale turbulent structures and has well-established equilibrium characteristics. On the other hand, the flow in the near wake is far from equilibrium. In this region, the oncoming boundary layer (which is rich in shear) is rapidly transformed into a free shear layer.

The few investigations of the near wake are of recent origin.¹⁻⁴ It is observed that, although the flow is not in equilibrium, the experimental results indicate some definite trends. Andreopoulos and Bradshaw¹ as well as Ramaprian et al.² have shown that the minimum mean velocity U_m in the near wake of a flat plate increases logarithmically with distance x along the flow as

$$\frac{U_m}{U^*} = A_1 \log_{10} \frac{xU^*}{\nu} + A_2$$

where A_1 and A_2 are constants, equal to 4.85 and 0.7, respectively, U^* the friction velocity of the boundary layer at the trailing edge of the flat plate, and ν the kinematic viscosity. Further, it is observed that, except for a short distance near the origin, the growth of the mixing layer follows the relation¹⁻⁴

$$(b/\theta)^2 = 0.225(x/\theta) + 11.0$$

where b is the half-width of the free shear layer and θ the momentum thickness far downstream, where its value is nearly constant. Slight variations in the values of the constants are observed among the results of different investigations. (See Fig. 3 below.)

Mixing layers could be formed with equal or different freestream velocities. The few studies under the latter condi-

tion^{5,6} are confined mainly to visualizing the flow in order to examine the instantaneous large-scale turbulence structures developed during the mixing process. The aim of the present investigation is to investigate the flowfield in the near-wake region of a flat plate with unequal freestream velocities. Apart from the experiments, attempts are being made to compute the mean velocity profiles in the near-wake region using the $K-\epsilon$ turbulence model.

Experimental Setup

The free mixing layer was produced behind a flat plate placed in the center of a rectangular duct as shown in Fig. 1. The plate was made of 15 mm thick polished wood, 200 cm long and 60 cm wide with a sharp trailing edge (3 deg wedge angle). Sand paper strips were placed on both sides of the plate to hasten and fix the location of the transition. In all of the experiments, the freestream velocity on the lower part of the duct (U_2) was maintained constant at 12.20 m/s, whereas the velocity on the other side of the plate (U_1) was varied by using screens of different porosities. Four velocity ratios U_1/U_2 , namely 0.32, 0.46, 0.74, and 0.96, were used in this investigation. The flow was produced by a low-noise blower. Between the duct and blower, a large settling chamber containing a honeycomb and a set of graded screens was incorporated to improve the quality of the flow. The duct was extended by about 100 cm downstream of the plate to contain the mixing layer without variation in the freestream velocities along x in the mixing zone. The mean velocities were measured with a hot wire operated in the constant-temperature mode.

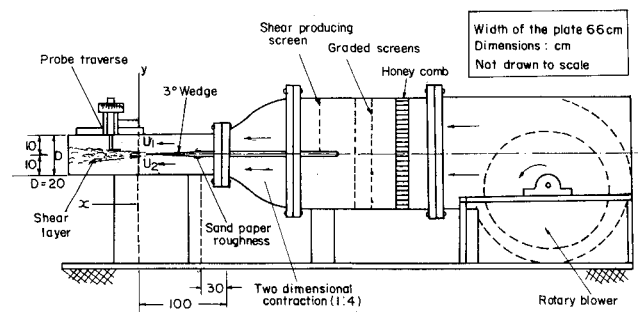


Fig. 1 Experimental setup.

Submitted Feb. 5, 1983; revision received Aug. 13, 1984. Copyright © American Institute of Aeronautics and Astronautics, Inc., 1984. All rights reserved.

*Professor, Department of Aerospace Engineering.

†Research Student, Department of Aerospace Engineering.

‡Assistant Professor, Department of Aeronautical Engineering.

Experimental Results and Discussion

The boundary layers at the trailing edge of the plate were turbulent in all of the experiments and exhibited a well-defined logarithmic region following the law of the wall,

$$U/U^* = 5.2 \log_{10} y U^* / \nu + 5.4$$

The thickness of the boundary layer δ was about 1.75 cm on both sides of the plate and remained nearly constant in the range of velocities used. Mean velocity profiles were measured in the mixing layer at a number of stations x up to $x = 80$ cm, which covered the entire near-wake region and a little beyond. The velocity profiles (Fig. 2) tend toward equilibrium as the flow moves downstream. However, the rate of adjustment seems to be faster for lower values of U_1/U_2 , a trend that could be attributed to the higher mixing rate when the velocity differences were large.

The half-width of the mixing layer b was estimated for $U_1/U_2 = 0.96$. For other cases, b could not be evaluated due to the very nature of the velocity profiles. Results show that the growth of the mixing layer follows the relation

$$(b/\theta)^2 = 0.225(x/\theta) + 10.5$$

θ is the momentum thickness at $x = 80$ cm, where the value of θ has almost reached a constant value independent of x . This relation is not valid very near the origin ($x/\theta < 30$) where the near wake is subjected to rapid changes in the process of transforming itself from a boundary-layer flow to a wake. Similar observations have been made by Ramaprian et al.² when they examined their results and those of others. All of the available data are shown in Fig. 3. There is good agreement between the results of the present experiments and those of Chevrey and Kovaznay³ and Pot.⁴ The other data^{1,2} indicate a well-defined logarithmic region with slight variations in the values of the constants. Since some ar-

bitrariness is involved in the estimation of θ , the discrepancy between the different results should not be considered as significant at present.

The changes in the mean velocity profiles in the near wake were examined by studying the variation of the minimum velocity U_m along x . For $U_1/U_2 = 0.96$, U_m occurred along the centerline ($y = 0$), whereas for the other three velocity ratios its location shifted toward the lower freestream velocity region of the mixing layer. The results are shown in Fig. 4 in the logarithmic form suggested earlier by Andreopoulos and Bradshaw,¹ namely

$$\frac{U_m}{U_a^*} = A_1 \log_{10} \frac{x U_a^*}{\nu} + A_2$$

Since the friction velocities on either side of the dividing plate were different, an average value $U_a^* = [(U_1^* + U_2^*)/2]$ was used in the present analysis. Well-defined logarithmic regions are observed for all four velocity ratios, the value of A_1 being nearly constant around 4.40 (Fig. 4). However, the value of A_2 is found to vary appreciably with U_1/U_2 . This logarithmic relation is somewhat similar to the law of the wall of a turbulent boundary layer, with the mean velocity across the boundary layer being replaced by U_m and the distance y from the wall by x . Such similarity exists because in both cases, there is relaxation of the flow from a higher shear region to a flow dominated by large-scale turbulence structures.

Computation of Mean Velocity Profiles

Houdeville and Tulapurkara⁷ found that the $K-\epsilon$ model of turbulence proposed by Jones and Launder⁸ satisfactorily predicts the development of symmetric and unsymmetric wakes with and without pressure gradients. In these cases, the external velocities on both sides of the wake are the

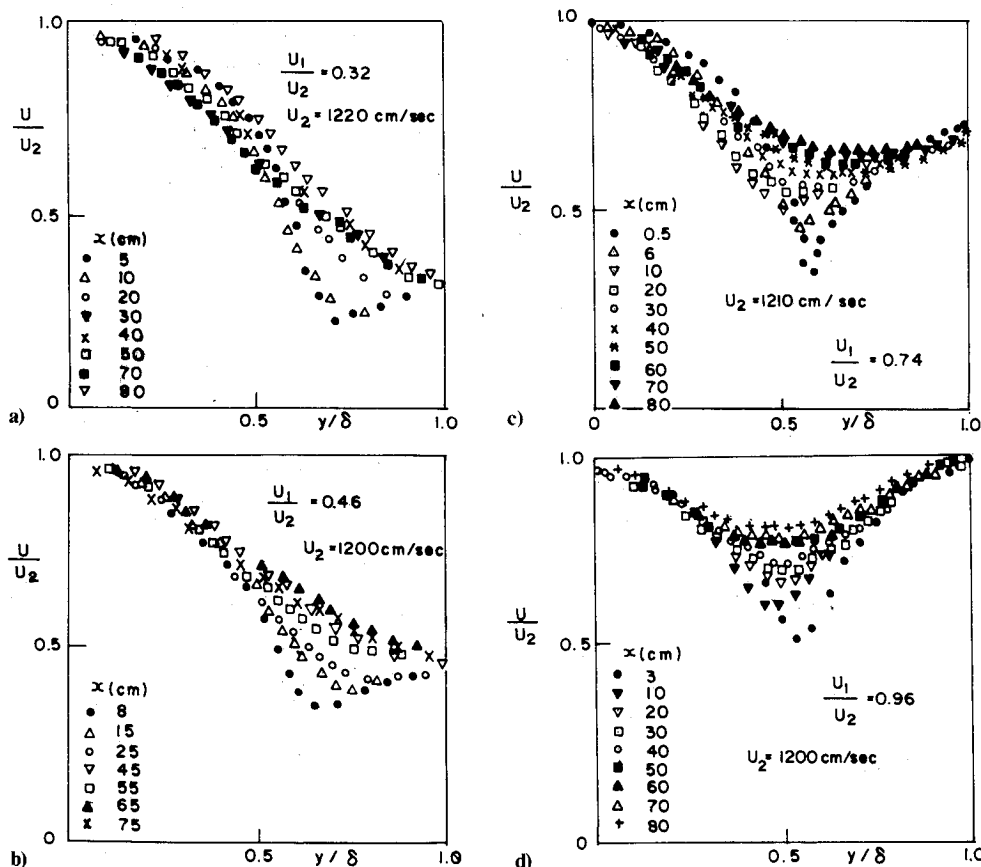


Fig. 2 Mean velocity profiles.

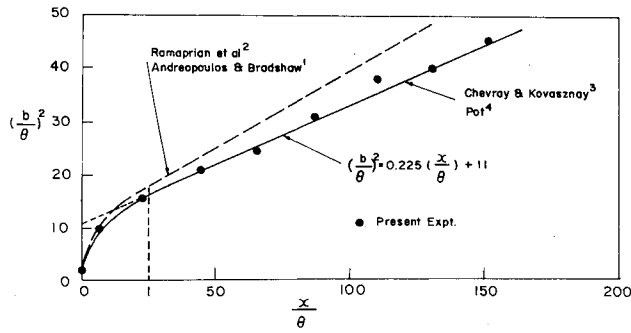
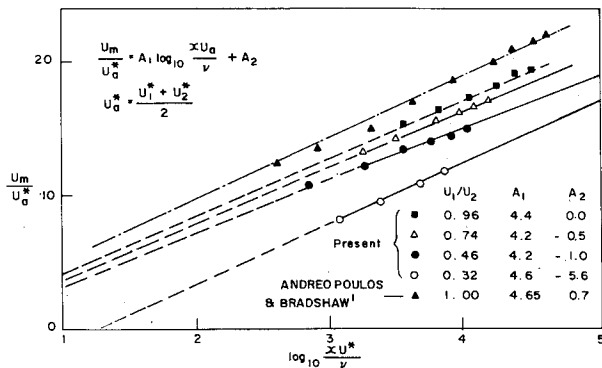
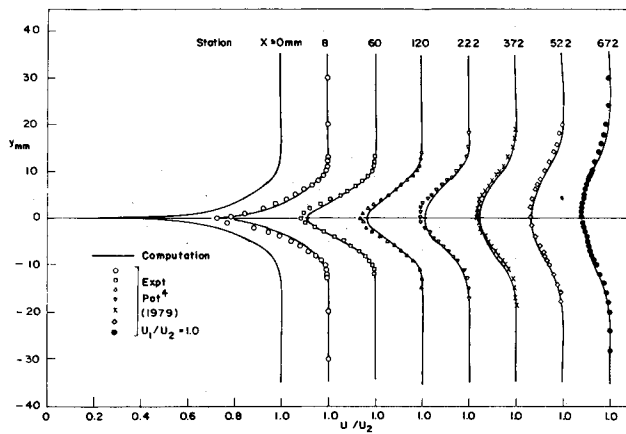
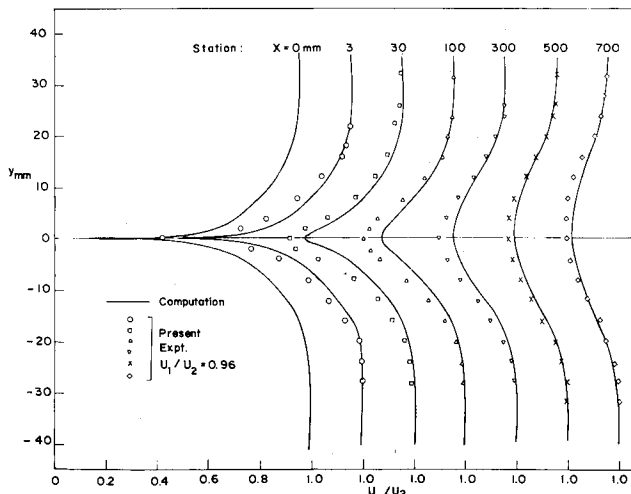


Fig. 3 Development of the mixing layer in similarity coordinates.

Fig. 4 Variation of minimum velocity along x with U_a^* as parameter.Fig. 5a Comparison of experiment and theory, $U_1/U_2 = 1.0$.Fig. 5b Comparison of experiment and theory, $U_1/U_2 = 0.96$.

same. Predictions with the same model are attempted in the present case where the external velocities are unequal. It may be added that Chien⁹ recently used a slightly different version of this model to predict channel flow and Baker et al.¹⁰ used a similar model successfully to compute the wake behind an airfoil.

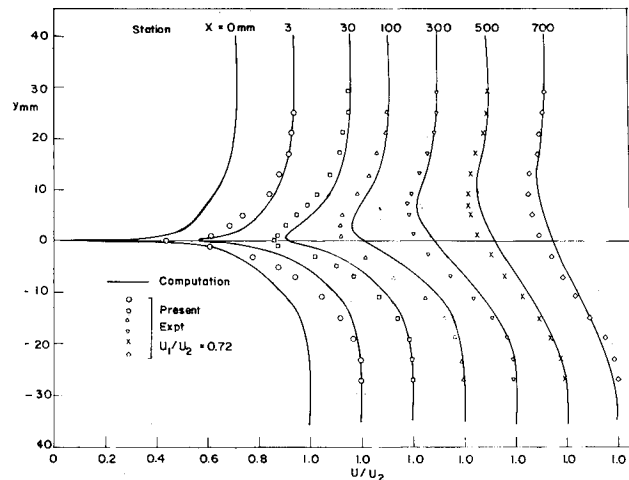
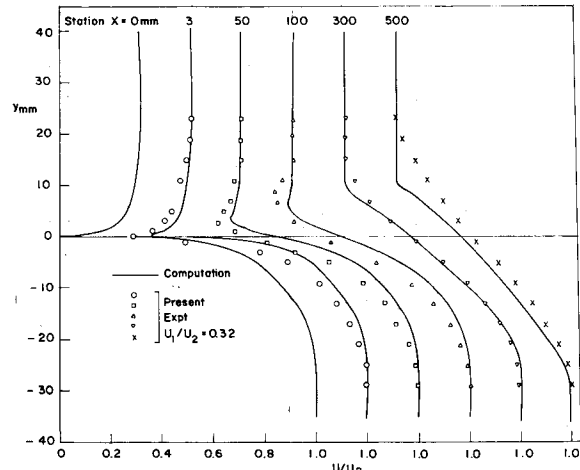
The basic governing equations are

$$U \frac{\partial U}{\partial x} + V \frac{\partial V}{\partial y} = 0 \quad (1)$$

$$U \frac{\partial U}{\partial x} + V \frac{\partial U}{\partial y} = U_0 \frac{\partial U_0}{\partial x} + \frac{\partial}{\partial y} \left(\frac{\partial U}{\partial y} - \overline{u'v'} \right) \quad (2)$$

$$U \frac{\partial K}{\partial x} + V \frac{\partial K}{\partial y} = -\overline{u'v'} \frac{\partial U}{\partial y} - \epsilon - 2\nu \left[\frac{\partial}{\partial y} (K^{1/2}) \right]^2 + \frac{\partial}{\partial y} \left[\left(\nu + \frac{\nu_t}{\sigma_k} \right) \frac{\partial K}{\partial y} \right] \quad (3)$$

$$U \frac{\partial \epsilon}{\partial x} + V \frac{\partial \epsilon}{\partial y} = \frac{\epsilon}{K} \left[C_{\epsilon 1} \overline{u'v'} \frac{\partial U}{\partial y} - f_2 C_{\epsilon 2} \epsilon \right] + 2\nu \nu_t \left(\frac{\partial U}{\partial y} \right)^2 + \frac{\partial}{\partial y} \left[\left(\nu + \frac{\nu_t}{\sigma_\epsilon} \right) \frac{\partial \epsilon}{\partial y} \right] \quad (4)$$

Fig. 5c Comparison of experiment and theory, $U_1/U_2 = 0.72$.Fig. 5d Comparison of experiment and theory, $U_1/U_2 = 0.32$.

where

$$\frac{u'v'}{U} = -\nu_t \frac{\partial U}{\partial y}; \quad \nu_t = f_\mu C_\mu \frac{K^2}{\epsilon}; \quad f_\mu = \exp\left[-\frac{2.5}{(1+R_t/50)}\right]$$

$$R_t = \frac{K^2}{\nu \epsilon}; \quad f_2 = 1 - 0.3 \exp(-R_t^2); \quad C_\mu = 0.09$$

$$\sigma_K = 1.0; \quad \sigma_\epsilon = 1.30; \quad C_{\epsilon_1} = 1.57; \quad C_{\epsilon_2} = 2.0$$

and where ν and ν_t are the kinematic and the eddy viscosities, respectively; U_0 the external freestream velocity (U_1 and U_2 in this case); U and V the mean velocities in the x and y directions, respectively; u' and v' the fluctuating velocity components of U and V , respectively; K the turbulence kinetic energy; and ϵ the rate of dissipation of K .

The above set of equations is parabolic. A numerical solution to this set is obtained using a computer code developed to calculate the development of the wake in external flow with a pressure gradient and unequal velocities on either side of the wake. The solution starts with the initial profiles of U , K , and ϵ . Then the transport equations for these three quantities are solved using the finite difference scheme of Patankar and Spalding.¹¹ The V component of the velocity is obtained taking $V=0$ at a suitable point and then numerically integrating the continuity equation.

The initial mean velocity profiles are generated from experimentally determined values of the momentum thickness θ and shape parameter H for the boundary layers at a station slightly ahead of the trailing edge of the dividing plate. Whitfield's¹² expressions for the turbulent boundary layer are employed for this purpose. This procedure is necessary to generate the smooth mean velocity profile required for computation. From the profiles of U , the profiles of K and ϵ are obtained using the expressions,

$$K = \left(F\ell \frac{\partial U}{\partial y}\right)^2 / 0.3 \quad (5)$$

$$\epsilon = (0.3K)^{1.5} / \ell \quad (6)$$

where

$$\ell = 0.085\delta \tanh\left(\frac{\chi}{0.085} \frac{y}{\delta}\right); \quad \chi = 0.41$$

$$F = 1.0 - \exp\left[-\left(\frac{\tau}{\rho}\right)^{1/2} \frac{\ell}{(26\chi\mu)}\right]; \quad \tau = \mu \frac{\partial U}{\partial y} \quad (7)$$

Here δ , τ , ρ , and μ are the boundary-layer thickness, shear stress, density, and coefficient of viscosity, respectively. The above expressions for ℓ and F are from Michel et al.¹³ Since V occurs in Eqs. (2-4), an initial profile for it is required to start the computation. This is obtained from the profile of U , using the continuity equation along with the similarity hypothesis that gives

$$\frac{\partial V}{\partial y} \cong \left(-\frac{U}{U_1}\right) \left(\frac{dU_1}{dx}\right)$$

With regards to the boundary conditions, we need to prescribe values of U , K , and ϵ along the upper and lower edges of the wake and V along a line in the shear layer. In the present investigation, the external velocities U_1 and U_2 , although unequal, remain constant with x . The values of the turbulent kinetic energy and rate of dissipation in the external flow (K_1 , K_2 and ϵ_1 , ϵ_2) are calculated using the following relations, which are the forms of Eqs. (3) and (4) in the external flow:

$$U_1 \left(\frac{dK_1}{dx}\right) = -\epsilon_1 \quad \text{and} \quad U_1 \left(\frac{d\epsilon_1}{dx}\right) = C_{\epsilon_2} \frac{\epsilon_1^2}{K_1} \quad (8)$$

The value of K_1 at the initial station is taken equal to the experimental value or equal to $0.0001 U_1^2$. The value of ϵ_1 at this station is calculated using Eq. (6). K_2 and ϵ_2 are calculated in a similar manner.

In a symmetric wake, V is equal to zero on the line of symmetry. But in the present asymmetric case the value of ordinate y (where V is equal to zero) varies with x . The influence of shifting the locations of the points where V is taken to be zero was examined for the case $U_1/U_2 = 0.72$. As a first step, $V=0$ was prescribed along a horizontal line starting from the trailing edge of the dividing plate. The computed velocity profiles for U are shown in Fig. 5c. Now, it can be reasonably assumed that the points where V equals zero would lie near the points where $U = U_{\min}$. Hence, velocity profiles were recalculated after prescribing $V=0$ along a line obtained by joining the points at which $U = U_{\min}$ at various stations along x . It was found that the maximum difference between these new profiles and those calculated in the first step was only 1% and the values of U_{\min}/U_1 at various stations, showed a change only in the third or fourth place of the decimal. Hence, it is concluded that the profiles of U are not very sensitive to where $V=0$ is prescribed. This is perhaps because the maximum value of V is only around 0.7% of U_1 . Since, as a matter of policy, iteration is avoided in the Patankar-Spalding scheme, the value of V in the present computations is taken equal to zero along a horizontal line passing through the trailing edge of the dividing plate in all cases. It may be added that Launder et al.¹⁴ have recently suggested that in the cases where the location of $V=0$ is not decided by the geometry of the flow, this location can be obtained by solving the equations for the V component of momentum and for $p(y)$.

Baker et al.¹⁰ have compared the experimental and the predicted profiles in the wake of a symmetric airfoil at zero angle of attack. Their comparison is confined to a very narrow regime between 0 and 0.1 chord length behind the airfoil. They found that the initial profiles have some influence on the predictions. During the course of their investigation, Houdeville and Tulapurkara⁷ examined this influence by using two different initial profiles of U and hence K , ϵ , and V . One profile was based on the Whitfield method¹² and the other on the local similarity hypothesis.¹⁵ The initial conditions were taken from the experimental data of Pot.⁴ It was observed that both the computed values were in very good agreement with the experimental results. U_m and θ differed from each other by less than 1% for a considerable distance ($x > 150\delta$). Thus, it is now firmly believed that as long as correct values of θ and H are used at the initial station, the mean velocity profiles in the free mixing layer can be computed with accuracy.

The grid for the finite difference scheme was formed as follows; the upper and the lower boundary layers are divided into N steps each and then five equidistance steps are added on either side. Thus, the total number of grid points are $(2N+9)$ as the central point is common to upper and lower boundary layers. As suggested by Cebeci and Smith,¹⁶ the step size in the boundary layers increases in geometric progression such that the ratio of the lengths of any two adjacent intervals is a constant. Thus, if $Y(J)$ is the ordinate of J th step, then

$$\frac{Y(J)}{\delta} = \frac{1 - Q^{J-1}}{1 - Q^{N-1}}$$

where δ is the boundary-layer thickness and Q the ratio of the lengths of intervals between steps. To study the influence of the grid size on the computed results, Q and N were varied. For this study, the symmetric wake data of Pot⁴ was used. As a first stage N was chosen as 50 and Q was varied between 1.04 and 1.14 in steps of 0.02. The changes in the velocity profiles were not noticeable on the scale of the graphs shown in Fig. 5. Integral values such as θ and b for

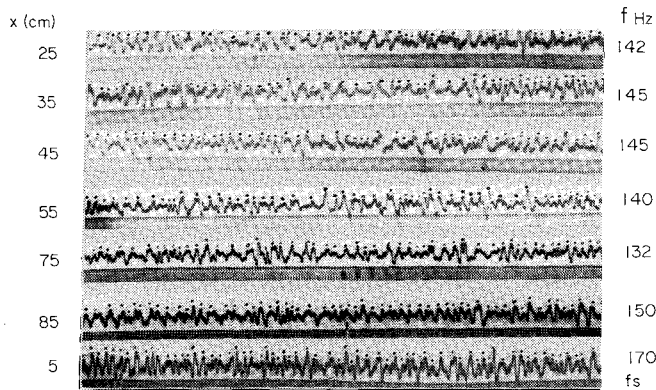


Fig. 6 Hot-wire signals along the centerline ($U_2 = 1220$ cm/s, $U_1/U_2 = 0.32$, $f_s \approx 140$).

all stations varied within 0.5% in the range of Q examined. Hence, $Q = 1.10$ was used in subsequent computations. In the second stage, N was varied from 30 to 60 in steps of 10 and the differences in the computed mean velocity profiles were again hardly noticeable. θ and b were slightly different between $N = 30$ and 40, but for $N = 40, 50$, and 60 the change was negligible. When this exercise was applied to $U_1/U_2 = 0.32$ (present experiment), the same conclusions were reached. Based on the above observation, a value of 50 for N was used in the subsequent computations.

About 1000 integration steps were needed to cover a distance of 700 mm. Initially, the step size was 2.5×10^{-3} mm, which was approximately doubled every 50th step until a step size of 1 mm was reached. Trials were carried out with initial step sizes of 10^{-2} , 5×10^{-3} , 2.5×10^{-3} , and 1.25×10^{-3} mm. The results for the last three cases were found to be almost identical. Typical execution time was 10 min of CPU time on an IBM 370 computer.

The computed mean velocity profiles are shown along with the experimental results of Pot and the present investigation in Fig. 5. It can be seen that the predicted minimum velocities are slightly higher and the width of the wake is slightly lower than the experimental values. However, considering the uncertainties involved in the measurement of mean velocities in a highly turbulent flow with a hot wire, the agreement between the two results can be considered as very satisfactory overall.

Periodic Fluctuations

While conducting the experiments, it was observed that the oscilloscope traces exhibited near-periodic signals when the hot-wire output was passed through a band pass filter allowing frequencies of 20-2000 Hz. These fluctuations were absent in the boundary-layer region as well as in the freestream. For $U_1/U_2 = 0.96$, the fluctuations were not clearly distinguishable, but became prominent as the velocity ratio was decreased. A photograph of the oscilloscope trace is shown in Fig. 6 for $U_1/U_2 = 0.32$. In this experiment, a single hot-wire was employed. It was kept inclined at 45 deg to the flow, so it was sensitive to both U and V . It is interesting to note that the frequency f_p of these fluctuations was nearly constant from $x = 5$ -85 cm. It is suspected that these signals might be the signature of the large-scale structures observed by Brown and Roshko⁵ in their experiments. Further study on this aspect of the free shear layers is being contemplated.

Conclusions

Experiments were conducted in the free mixing region of two parallel streams with unequal velocities and with turbulent boundary layers at the origin. In the near wake, the

minimum mean velocity U_m was found to follow the law

$$\frac{U_m}{U_a^*} = A_1 \log_{10} \frac{x U_a^*}{\nu} + A_2$$

The value of A_1 was nearly constant at 4.4 ± 0.2 for all cases, whereas A_2 varied with the velocity ratio. In the flow for which the freestream velocity ratio was 0.96, the growth of the shear layer followed the relation $(b/\theta)^2 = 0.225(x/\theta) + 11.0$. There was good agreement between the measured mean velocity profiles and those computed using $K-\epsilon$ turbulence model. Distinct large-scale fluctuations were observed in the hot-wire traces and they persisted for appreciable distances downstream in the mixing layer; their rate of occurrence remaining nearly constant with x . Nearly periodic fluctuations were observed in the hot-wire traces when the signal from the wire was passed through a band pass filter allowing frequencies of 20-2000 Hz. The frequency of these fluctuations was constant along the flow for a considerable distance.

Acknowledgments

The third author is thankful to his colleagues Dr. T. K. Bose and Dr. G. Subramanian for many useful discussions during the course of computations.

References

- Andreopoulos, J. and Bradshaw, P., "Measurement of Interacting Turbulent Shear Layers in the Near Wake of a Flat Plate," *Journal of Fluid Mechanics*, Vol. 100, 1980, pp. 639-668.
- Ramaprian, B. R., Patel, V. C., and Sastry, M. S., "Symmetric Turbulent Wake of a Flat Plate," *AIAA Journal*, Vol. 20, 1982, pp. 1228-1235.
- Chevray, R. and Kovaszny, L. S. G., "Turbulence Measurements in the Wake of a Thin Flat Plate," *AIAA Journal*, Vol. 7, 1969, pp. 1641-1643.
- Pot, P. J., "Measurements in a 2-D Wake and in a 2-D Wake Merging into a Boundary Layer," NLR, the Netherlands, Data Rep. TR-79063 U, 1979.
- Brown, G. L. and Roshko, A., "On Density Effects and Large Structure in Turbulent Mixing Layers," *Journal of Fluid Mechanics*, Vol. 85, 1978, pp. 693-704.
- Browand, F. K. and Weidmann, P. D., "Large Scales in the Developing Mixing Layer," *Journal of Fluid Mechanics*, Vol. 76, 1976, pp. 127-144.
- Houdeville, R. and Tulapurkara, E. G., "Prediction of Boundary Layers, Wakes and Mixed Flows Using a Modified $K-\epsilon$ Model," ONERA, CERT, Rapport Technique OA 46/2259, June 1981.
- Jones, W. P. and Launder, B. E., "The Prediction of Relaminarization with Two Equation Model of Turbulence," *International Journal of Heat and Mass Transfer*, Vol. 15, 1972, pp. 301-314.
- Chien, K. Y., "Prediction of Channel and Boundary-Layer Flows with a Low Reynolds Number Turbulence Model," *AIAA Journal*, Vol. 20, Jan. 1982, pp. 33-38.
- Baker, A. J., Yu, J. C., Orzechowski, J. A., and Gatski, T. B., "Prediction and Measurement of Incompressible Turbulent Aerodynamic Trailing Edge Flows," *AIAA Journal*, Vol. 20, Jan. 1982, pp. 51-59.
- Patankar, S. V. and Spalding, D. B., "A Finite Different Procedure for Solving the Equations of Two-Dimensional Boundary Layer," *International Journal of Heat and Mass Transfer*, Vol. 10, 1967, pp. 1389-1411.
- Whitfield, D. L., "Analytical Description of the Complete Turbulent Boundary Layer Velocity Profiles," *AIAA Journal*, Vol. 17, 1979, pp. 1145-1147.
- Michel, R., Quemard, C., and Durant, R., "Application d'un schéma de longueur de mélange à l'étude des couches limites d'équilibre," ONERA, NT 154, 1969.
- Launder, B. E., Leschziner, M. A., and Sindir, M., "Comparison of Computation with Experiment," *Proceedings of the 1980-81 AFOSR-HTTM-Stanford Conference on Complex Turbulent Flows*, Vol. III, Stanford University, Stanford, Calif., 1982.
- Houdeville, R. and Cousteix, J., "Couches limites turbulentes bidimensionnelles avec flux de chaleur-D-Programme de calcul de solutions de similitude," ONERA, CERT DERAT, NT 6/5005, June 1974.
- Cebeci, T. and Smith, A. M. O., *Analysis of Turbulent Boundary Layers*, Academic Press, New York, 1974.